MIT Libraries | DSpace@MIT

MIT Open Access Articles

Mechanisms that promote the evolution of cross-reactive antibodies upon vaccination with designed influenza immunogens

The MIT Faculty has made this article openly available. ***Please share*** how this access benefits you. Your story matters.

Citation: Yang, Leerang, Caradonna, Timothy M, Schmidt, Aaron G and Chakraborty, Arup K. 2023. "Mechanisms that promote the evolution of cross-reactive antibodies upon vaccination with designed influenza immunogens." Cell Reports, 42 (3).

As Published: 10.1016/j.celrep.2023.112160

Publisher: Elsevier BV

Persistent URL: https://hdl.handle.net/1721.1/157801

Version: Final published version: final published article, as it appeared in a journal, conference proceedings, or other formally published context

Terms of use: Creative Commons Attribution-NonCommercial-NoDerivs License

Massachusetts Institute of Technology

Cell Reports

Article

Mechanisms that promote the evolution of cross-reactive antibodies upon vaccination with designed influenza immunogens

Graphical abstract

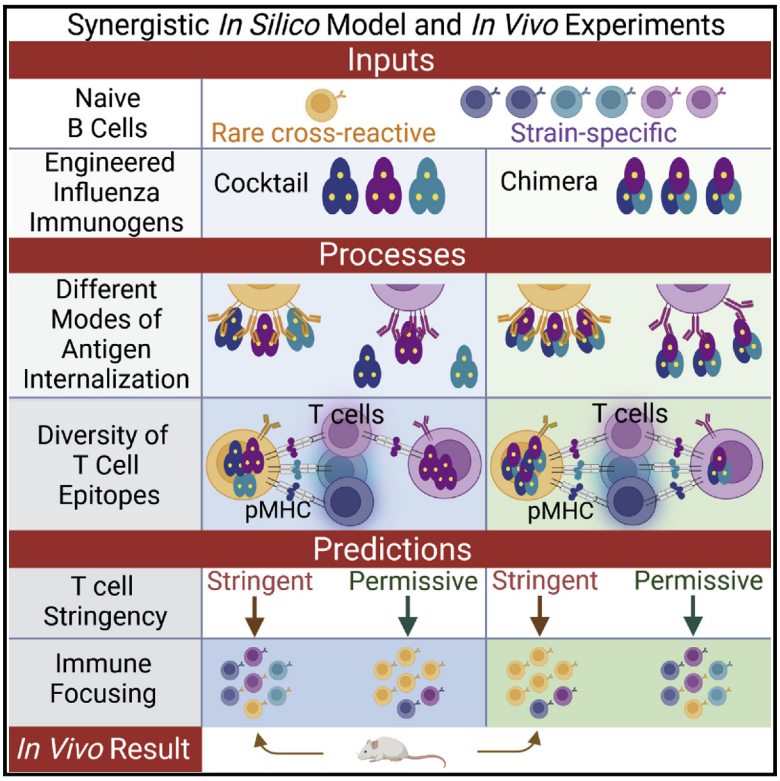

Highlights

- Engineered influenza immunogens can elicit cross-reactive antibodies
- Chimeric design results in better antigen capture by cross-reactive GC B cells
- Cocktail immunogens allow cross-reactive GC B cells to interact with diverse T cells
- Chimera elicits more cross-reactive GC B cells when T cell selection is stringent

Authors

Leerang Yang, Timothy M. Caradonna, Aaron G. Schmidt, Arup K. Chakraborty

Correspondence

arupc@mit.edu

In brief

Yang et al. describe the mechanisms underlying differences between how two engineered influenza hemagglutinin immunogens elicit broadly cross-reactive antibodies targeting a conserved epitope. The results are consistent with *in vivo* experiments, and the observations aid in the design of universal influenza vaccines and further our understanding of cross-reactive antibody development.

Yang et al., 2023, Cell Reports *42*, 112160
March 28, 2023 © 2023 The Author(s).
https://doi.org/10.1016/j.celrep.2023.112160

CellPress

Cell Reports

CellPress
OPEN ACCESS

Article

Mechanisms that promote the evolution of cross-reactive antibodies upon vaccination with designed influenza immunogens

Leerang Yang,[1] Timothy M. Caradonna,[2] Aaron G. Schmidt,[2,3] and Arup K. Chakraborty[1,2,4,5,6,7,*]
[1]Department of Chemical Engineering, Massachusetts Institute of Technology, Cambridge, MA 02139, USA
[2]Ragon Institute of MGH, MIT, and Harvard, Cambridge, MA 02139, USA
[3]Department of Microbiology, Harvard Medical School, Boston, MA 02115, USA
[4]Department of Physics, Massachusetts Institute of Technology, Cambridge, MA 02139, USA
[5]Department of Chemistry, Massachusetts Institute of Technology, Cambridge, MA 02139, USA
[6]Institute of Medical Engineering and Science, Massachusetts Institute of Technology, Cambridge, MA 02139, USA
[7]Lead contact
*Correspondence: arupc@mit.edu
https://doi.org/10.1016/j.celrep.2023.112160

SUMMARY

Immunogens that elicit broadly neutralizing antibodies targeting the conserved receptor-binding site (RBS) on influenza hemagglutinin may serve as candidates for a universal influenza vaccine. Here, we develop a computational model to interrogate antibody evolution by affinity maturation after immunization with two types of immunogens: a heterotrimeric "chimera" hemagglutinin that is enriched for the RBS epitope relative to other B cell epitopes and a cocktail composed of three non-epitope-enriched homotrimers of the monomers that comprise the chimera. Experiments in mice find that the chimera outperforms the cocktail for eliciting RBS-directed antibodies. We show that this result follows from an interplay between how B cells engage these antigens and interact with diverse helper T cells and requires T cell-mediated selection of germinal center B cells to be a stringent constraint. Our results shed light on antibody evolution and highlight how immunogen design and T cells modulate vaccination outcomes.

INTRODUCTION

The mutability of viruses like human immunodeficiency virus (HIV) and influenza poses a major public health challenge. No effective vaccine is available for HIV, and seasonal variation of influenza requires annual vaccine reformulation. Additionally, severe acute respiratory syndrome coronavirus 2 (SARS-CoV-2) is rapidly evolving variants that reduce the efficacy of current vaccines, raising the possibility that booster shots may be required periodically.[1,2] Developing vaccines that can induce broadly neutralizing antibodies (bnAbs) against highly mutable pathogens could address these challenges. BnAbs can neutralize diverse mutant strains by targeting relatively conserved regions on viral surface-exposed proteins. Although bnAbs for HIV[3–5] and influenza[6–8] have been identified, their natural development is typically rare and delayed.[9,10] Therefore, significant efforts are devoted to designing immunogens[11–13] or vaccination regimens[14,15] that may elicit bnAbs with the ultimate goal of creating so-called "universal" vaccines. The complexity of this challenge has also motivated several theoretical and computational studies focused on the mechanisms underlying bnAb evolution.[16–26]

Upon natural infection or vaccination, antibodies are elicited through a Darwinian evolutionary process called affinity maturation.[27] Naive B cells that express a B cell receptor (BCR) with sufficiently high affinity for an antigen, such as a viral protein, can seed germinal centers (GCs). GC B cells multiply and diversify their BCRs through somatic hypermutation and subsequently interact with the antigen presented on follicular dendritic cells (FDCs). GC B cells internalize varying amounts of antigen based on the binding affinity of their BCRs to the cognate antigen and then display peptides derived from the antigen complexed with major histocompatibility complex (MHC) class II molecules (pMHC complexes) on their surfaces.[28] These B cells compete to interact with helper T cells. Productive interactions result in positive selection that leads to proliferation and mutation, while failure to obtain sufficient help signal triggers B cell apoptosis. Many rounds of mutation and selection ensue, resulting in a progressive increase in B cell binding affinity; some B cells differentiate into memory B cells and plasma cells that produce antibodies.[29]

BnAb evolution is rare upon natural infection for at least two reasons. First, the frequency of germline B cell precursors that target conserved epitopes is low.[30] Many germline B cells that target highly variable regions on the antigen can co-seed GCs and ultimately outcompete rare B cells that recognize the conserved epitope during affinity maturation.[31] Second, the conserved epitope-directed B cell precursors may acquire

This is an open access article under the CC BY-NC-ND license (http://creativecommons.org/licenses/by-nc-nd/4.0/).

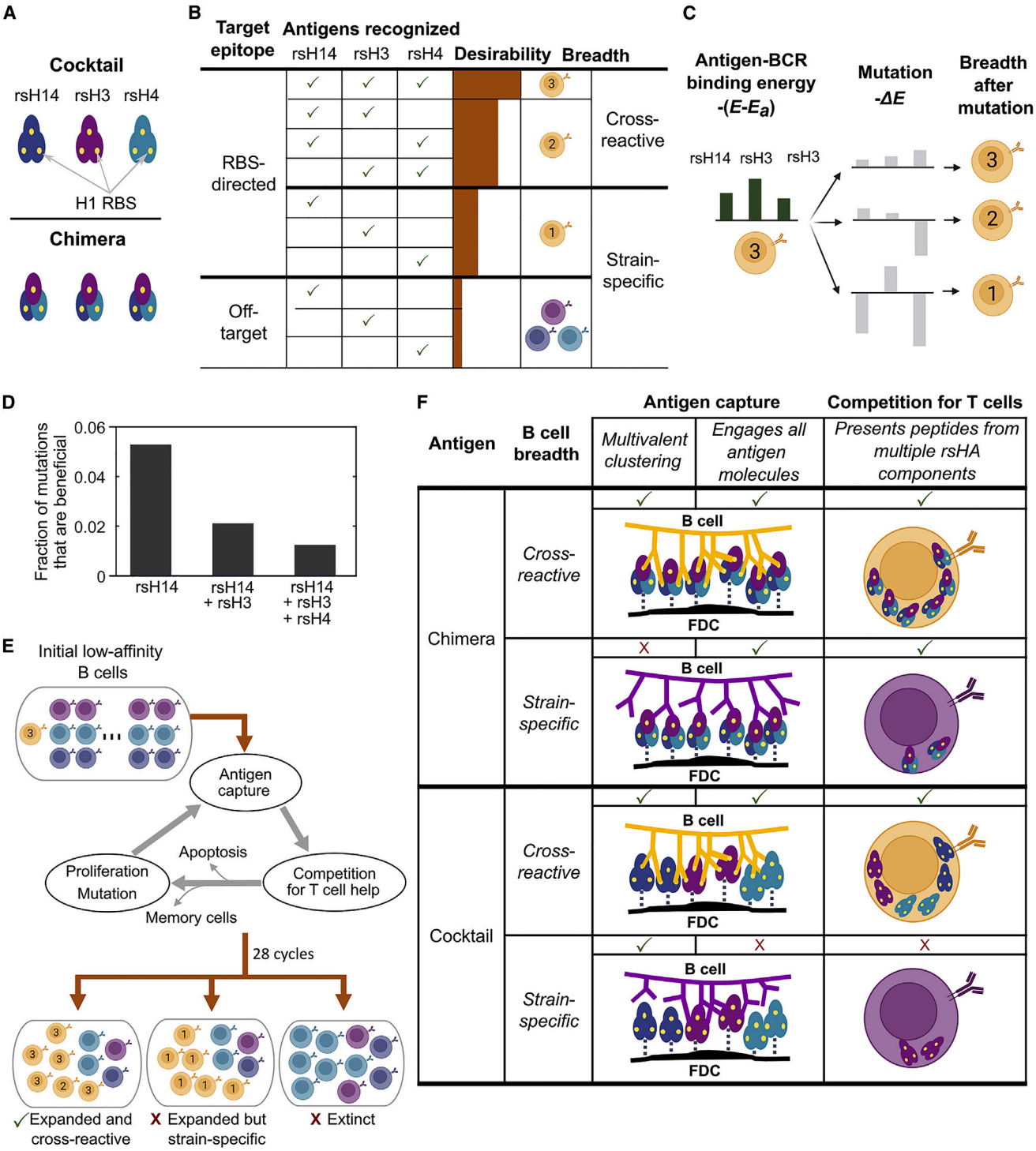

Figure 1. Schematics of the study design

(A) Schematic of the two rsHA immunogen designs: the cocktail of three rsHA homotrimers and the heterotrimeric "chimera."

(B) Classifications of the GC B cells based on their target epitopes as RBS directed or off target and based on their breadths as cross reactive or strain specific; an RBS-directed B cell can bind three, two, or one of the rsHA components, and an off-target B cell can only bind one of the three components.

(C) Schematic of how a mutation can alter the breadth of an RBS-directed B cell.

(D) Fraction of affinity-changing mutations in the simulations that are beneficial for one or two specific rsHA components or all three. Interchanging the specific rsHA components referred to in the panel yields the same result.

(legend continued on next page)

"specializing" mutations and lose their breadth of coverage during affinity maturation.[16,32,33] Specialization can occur when the BCR binding footprint is larger than the exposed conserved region on the antigen epitope, which is true for HIV and influenza RBS epitopes.[32,34] In this case, the BCR can develop strong interactions not with the conserved residues but with the variable residues surrounding them. Therefore, an engineered immunogen that selectively enriches rare B cell precursors for the conserved epitope and also guides them to acquire mutations that promote high breadth is necessary for eliciting bnAbs.

Here, we develop a computational model to study the mechanisms that influence the evolution of influenza RBS-directed B cells during affinity maturation. Toward this goal, we study the relative efficacy of RBS-directed B cell evolution upon vaccination with two different types of designed immunogens.[35] Both immunogens are "resurfaced" hemagglutinin (rsHA) immunogens, where the RBS epitope of H1 A/Solomon Islands/03/2006 (H1 SI-06) is grafted onto antigenically distinct H3, H4, and H14 HA head scaffolds (Figure 1A).[36] The first type of immunogen is an rsHA trimeric "chimera," a cystine-stabilized rsH3-rsH4-rsH14 heterotrimer, each presenting the same H1 SI-06 RBS epitope; because of the antigenic distance between the H3, H4, and H14 scaffolds, the RBS epitope is enriched relative to all other epitopes.[37] The second type is a cocktail of non-epitope-enriched homotrimers of each rsHA; this cocktail contains the same rsHA monomers as the chimera but as homotrimers rather than a single heterotrimer.

Caradonna et al.[35] report that immunization with the chimera and cocktail immunogens in mice elicit cross-reactive RBS-directed B cells, but the chimera qualitatively outperforms the cocktail. Our computational results reveal the mechanism underlying this result. By studying these complex immunogens, we show how the outcome of GC processes is determined by the interplay of multiple factors: how B cells engage with these immunogens and internalize antigen, the diversity of helper T cells with which GC B cells can interact, and the stringency of helper T cell-mediated selection. We find that, upon immunization with the cocktail of homotrimers, only the cross-reactive B cells can interact with T cells of diverse specificities, while the strain-specific B cells must rely on a restricted set of helper T cells. In contrast, upon immunization with the chimeric heterotrimer, cross-reactive and strain-specific B cells can interact with T cells of diverse specificities. So, intuition may lead us to the conclusion that immunization with the cocktail of homotrimers should perform better than the chimeric heterotrimer at promoting the evolution of cross-reactive B cells. The experiments show that the opposite is true. This is because, upon immunization with the chimera, the cross-reactive B cells internalize far more antigen than the strain-specific B cells in the early GCs, while these two types of B cells internalize similar amounts of antigen upon immunization with the cocktail. We show that the chimera performs better as a result of more effective antigen internalization coupled with helper T cells stringently discriminating between B cells based on the amount of pMHC displayed.

Previously, Gitlin et al.[38] showed that T cell help is a stringent constraint on the selection of GC B cells, while another study suggested that this was not so.[39] Our finding that T cell help must be a stringent constraint on B cell evolution in the GC helps resolve this debate. Furthermore, these data highlight the importance of immunogen design and helper T cells in determining vaccination outcomes and suggest that modulating these effects is necessary to elicit influenza RBS-directed B cells with breadth.

RESULTS

Model development

Overview of the model

We simulate GC reactions induced by either the cocktail or the chimera immunogens, described above and in Caradonna et al.[35] The GC B cells that bind to these antigens are classified as either "RBS directed" or "off target." The three HA scaffolds are antigenically distinct; the sequence homologies between the rsHA components are ~58.4% (rsH3-rsH4), ~60.5% (rsH3-rsH14), and ~72.5% (rsH4-rsH14). These values are comparable with or lower than the HA sequence homology of ~70.8% between a pandemic influenza strain and a previous strain (H1N1 A/California/4/2009 and H1N1 A/Solomon Islands/3/2006) and are much lower than the typical sequence homology resulting from antigenic drift (e.g., ~95.4% between H1N1 A/New Caledonia/20/1999 and H1N1 A/Solomon Islands/3/2006). Therefore, while it may not be impossible for off-target B cells to develop cross-reactivity toward multiple rsHA components, such cases are likely very rare. In our model, we assume that an off-target B cell is always strain specific and can only target one of the rsHA components (Figure 1B).

An RBS-directed B cell can potentially target all three components because of the similarities of the resurfaced RBS regions. However, because the grafted RBS is smaller than the typical footprint of a BCR, we account for the fact that RBS-directed B cells must contact peripheral residues that are variable. Thus, different RBS-directed B cells may have different breadths in our model, as summarized in Figure 1B. A mutation changes the binding free energies of an RBS-directed B cell for the three rsHA components differently (Figure 1C). These changes are drawn from a positively correlated probability distribution to account for the similarities of the RBS regions. However, some mutations will be beneficial for binding to one or two rsHA components and deleterious for the others (Figure 1D). As affinity maturation progresses, the affinities of an RBS-directed B cell for the three components can vary and even fall below the recognition threshold for some components.

Figure 1E describes the process that occurs in GCs. Because off-target germline B cells outnumber the RBS-directed germline B cells,[32,40] we seed each GC with 99 off-target B cells and 1 RBS-directed B cell, making the total founder number

(E) Schematic of the affinity maturation simulation and three general possible outcomes of the GCs. The most desirable outcome is that the rare RBS-directed B cells are expanded, and the descending B cells are cross reactive.
(F) Schematics that summarize how the designs of the two immunogens affect the abilities of cross-reactive and strain-specific B cells to capture antigen and compete for T cell help. See the main text for details.

representative of GCs in mice.[41] Each off-target B cell is randomly assigned a single rsHA target at the beginning of the simulation. To model the GC dynamics in mice, founder B cells divide four times without mutation, and then the competitive phase of affinity maturation lasts for 28 cycles, or ~14 days.[29,42] These B cells undergo cycles of antigen capture and competition for T cell help. In each cycle, B cells that fail positive selection are subsequently removed from the GC via apoptosis. Additionally, ~10% of positively selected B cells stochastically differentiate into memory and plasma cells and exit the GC. The remaining positively selected B cells divide twice,[43] and one daughter cell mutates in each division.[44]

In this study, we ask how the design of an immunogen affects its ability to expand the RBS-directed B cells in GCs and to shepherd them to acquire mutations that confer cross-reactivity. Undesirable alternative outcomes are that RBS-directed B cells become outcompeted by off-target B cells or that they become strain specific by acquiring specializing mutations (Figure 1E). The chimera and cocktail immunogens give advantages to cross-reactive B cells over strain-specific B cells in different ways during the antigen capture and T cell help steps, as summarized in Figure 1F. The chimera antigen presented on the FDC during the antigen capture step can form multivalent clusters with cross-reactive B cells but not with strain-specific B cells. This is because a cross-reactive RBS-directed B cell can bind to a single chimera molecule with up to three BCRs, but a strain-specific B cell can bind to a single chimera molecule with, at most, one BCR. Then, during the competition for T cell help, cross-reactive and strain-specific B cells that capture the chimera can present peptides from all three rsHA components (Figure 1F).

In contrast, after cocktail immunization, cross-reactive B cells and strain-specific B cells can engage a single antigen trimer with multiple BCRs and thus form multivalent clusters between BCRs and antigen molecules. However, the strain-specific B cells can only recognize a third of the total antigen molecules. Then, during the competition for T cell help, only the cross-reactive B cells present peptides from multiple rsHA components, while strain-specific B cells only present the peptides from the single component they target (Figure 1F).

Initial condition and mutation of B cells

The initial free energy of binding (or affinity) is set to be E_a for the target rsHA component for the off-target B cells. For simplicity, the RBS-directed precursors are assumed to initially bind all three components with affinity E_a. The absolute value of E_a does not affect the results because all other free energies are scaled to this reference. We choose $E_a = -13.8\ k_BT$, where k_B is the Boltzmann constant, and T is the temperature (~300 K), because it corresponds to a dissociation constant, K_D, of 1 μM, which is approximately the threshold for naive B cell activation.[45]

A mutation is fatal, silent, or affinity changing with probabilities of 0.3, 0.5, and 0.2, respectively.[46] The Protein-protein Interactions Thermodynamics (PINT) database shows that affinity changes of protein-protein interfaces upon mutations are more likely to decrease than to increase the binding affinity.[47] We describe these data using a shifted log-normal distribution; for an off-target B cell, i, the free energy change because of mutation is given by

$$\Delta E_i = e^{\mu + \sigma Y} - \delta \quad \text{(Equation 1)}$$

where Y is a standard normal random variable, and μ, σ, and δ are parameters chosen so that about 5% of the mutations are beneficial.[16,18]

For RBS-directed B cells, a mutation changes the binding affinities toward the rsHA components differently. However, the marginal distribution of affinity change toward any one component should be equivalent to that of an off-target B cell mutation. To model this, we draw three random numbers, $\bar{y} = [y_1, y_2, y_3]$, one for each component, from a multivariate Gaussian distribution with the mean of zero and the covariance matrix of Λ, as follows:

$$\bar{y} \sim \frac{\exp\left(-\frac{1}{2}\bar{y}^T \Lambda^{-1} \bar{y}\right)}{\sqrt{(2\pi)^3 |\Lambda|}} \quad \text{(Equation 2)}$$

Where $\Lambda = \begin{bmatrix} 1 & \rho & \rho \\ \rho & 1 & \rho \\ \rho & \rho & 1 \end{bmatrix}$. Choosing the correlation, ρ, to be smaller than 1 allows us to study the effects of the mutations that make B cells specialize to a subset of rsHA components. For a given RBS-directed B cell, I, each sampled number, y_j, corresponding to the rsHA component, j, is then converted to the free energy change because of mutation, ΔE_{ij}, for this variant analogous to Equation 1 as follows:

$$\Delta E_{ij} = e^{\mu + \sigma y_j} - \delta \quad \text{(Equation 3)}$$

We chose $\rho = 0.7$; we also carried out calculations with $\rho = 0.4$, and the qualitative findings are not affected by this change. In Equation 2, by using symmetric Λ, we treat the antigenic differences between the RBS epitopes of the three rsHA components as equidistant. Because the RBS is grafted on to the scaffold, the variations among the RBS epitopes should be smaller than the differences between the scaffolds and not directly correlated to them. For simplicity, and because the qualitative findings of the study do not depend on changing ρ, we use the same value for each pair.

Antigen capture by B cells

GC B cells extract antigens from the surfaces of FDCs using mechanical pulling forces.[28,48] The B cell synapse interacting with an FDC is modeled as a 2-dimensional circle divided into lattice points occupied by antigen molecules and BCRs.[49,50] BCRs and antigen molecules are initially randomly distributed on the lattice. The lattice spacing is 10 nm, which is of the same order as the collision radius of BCR and ligand.[50] During the clustering phase, BCR and antigen molecules diffuse freely and attempt to bind when they are within one lattice point (see STAR Methods for details). The probability of success is

$$p_{on} = 1 - e^{-q_{on}\Delta t \cdot [E_{ij} \le E_a]} \quad \text{(Equation 4)}$$

where the Iverson bracket sets the minimum affinity required for binding to be E_a, which is equal to the initial B cell affinity, and

$$q_{on} = q^0_{on} n_{arm} n_{ep} \quad \text{(Equation 5)}$$

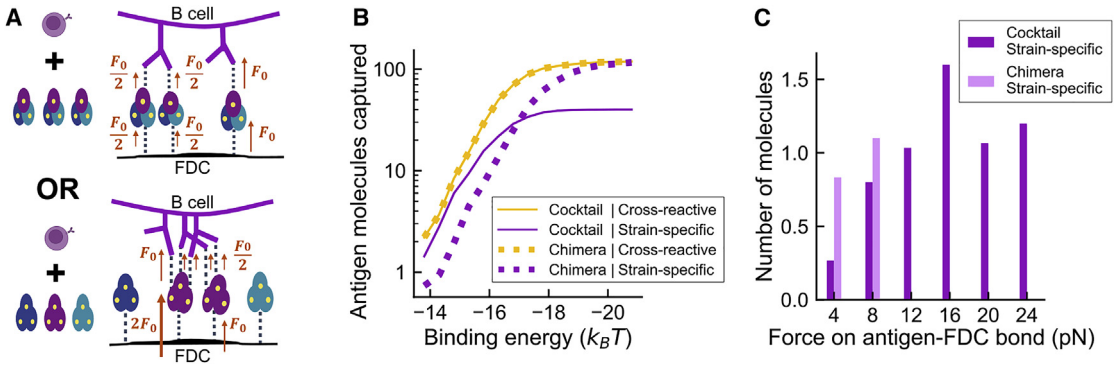

Figure 2. Effect of immunogen design on antigen capture by B cells

(A) Schematics of force-based antigen extraction by a strain-specific B cell. For the chimera, the only two possible configurations of antigen and BCR interactions are shown. For the cocktail, an example of many possible configurations of BCR-antigen clusters is shown. For the heterotrimeric chimera, one antigen molecule can be bound by only one BCR, so the pulling force on the antigen-FDC bond is always equal to the pulling force on the antigen-BCR bond. For the homotrimer molecules in the cocktail, multiple BCRs can pull on the same cognate antigen molecule so that greater force accumulates on the antigen-FDC bond.

(B) Amount of antigen captured as a function of antigen-BCR binding affinity. For the cross-reactive B cell, when the binding affinity toward all three rsHA components is equal is shown.

(C) Histogram of the forces on antigen-FDC bonds when either the cocktail or the chimera antigen molecules are extracted by a strain-specific B cell of low affinity ($-14.8\ k_BT$).

(B) and (C) were constructed by taking the mean value from 30 simulations. See also Figure S1.

represents the steric factor. This factor is determined by n_{arm}, the number of free BCR arms (between 0 and 2); n_{ep}, the number of free cognate BCR epitopes on the antigen (between 0 and 3); and the basal rate $q_{on}^0 = 10\ s^{-1}$. With $\Delta t = 5 \times 10^{-4}$ s, which is the characteristic timescale of diffusion over the lattice, this basal rate results in the successful binding probability of $p_{on} = 5 \times 10^{-3}$. This number approximately accounts for the entropic penalty of aligning two molecules.

An established antigen-BCR bond (labeled i below) breaks with probability

$$p_i^{off} = 1 - e^{-k_i^{off}\Delta t} \quad \text{(Equation 6)}$$

where k_i^{off} is its off-rate. Assuming that the activation barrier for bond formation is negligible compared with the binding free energy, the off-rate is related to binding free energy by

$$k_i^{off} = k_0^{off} e^{\frac{E_{ij}}{k_BT}} \quad \text{(Equation 7)}$$

where E_{ij} is the binding free energy of BCR, i, for antigen j, and $k_0^{off} = 10^6\ s^{-1}$.[45]

Our simulations result in formation of antigen-BCR clusters, dependent on the cross-reactivity of the B cell and the design of the antigen. The clustering is followed by antigen internalization through mechanical pulling. We assume that antigen molecules are tethered to the FDC membrane with a binding free energy of $-19\ k_BT$, which makes antigen capture most sensitive to affinity change in K_D of 1–0.01 μM range, but the affinity ceiling is reached when $K_D << 1$ nM.[45] A pulling force of 8 pN is applied to each BCR,[28] which is transferred to the antigen-BCR bonds and the antigen-FDC bonds,[51] as schematically shown in Figure 2A. If a BCR is bound to 2 antigen molecules, then the force is divided equally by the two arms of the BCR. For a given antigen molecule, the force applied to its antigen-FDC bond is the sum of forces applied by all the BCR arms bound to it. The off-rates of antigen-FDC and antigen-BCR bonds increase with the applied force[52]

$$k_F^{off} = k^{off} \times \exp\left(\frac{x_b F}{k_B T}\right) \quad \text{(Equation 8)}$$

where k_F^{off} is the off-rate under force, F is the force, and x_b is the bond length, taken to be 1 nm.[53] When an antigen-BCR bond breaks, the BCR goes into a refractory state, which prevents instant rebinding with the same antigen.[53] The duration is taken to be 0.1 s, which is much greater than the antigen diffusion timescale of 5×10^{-4} s (STAR Methods). At the end of each time step, any BCR or antigen-BCR cluster that is not connected to the FDC is internalized.

Competition for helper T cells

Briefly, after the antigen capture step, B cells present peptides derived from each rsHA component they have captured, in proportion to the amount captured. We developed a model that accounts for B cells competing for selection by helper T cells based on the types and amounts of peptides they present. We discuss this in more detail later.

Antigen capture depends on immunogen design and cross-reactivity of B cells

Figure 2B shows the total amount of antigen captured as a function of BCR binding affinity for cross-reactive and strain-specific B cells, capturing the cocktail or the chimera immunogen. Notably, neither immunogen design is better at conferring an advantage to RBS-directed B cells in capturing antigens across the entire affinity range. At low affinity, representative of the early GC, the advantage of cross-reactive B cells over strain-specific B cells is greater for the chimera. At high affinity, the opposite is true.

At low affinity, antigen availability is not limiting, and the amount of antigen captured is largely determined by the forces imposed on the antigen-FDC bonds by the BCRs bound to the antigen molecules. A strain-specific B cell can engage a homotrimeric antigen in the cocktail with multiple BCRs but not the chimera (Figures 1F and S1A). Therefore, the forces on the antigen-FDC bonds are typically higher for the homotrimeric antigen bound by strain-specific B cells compared with the chimera bound by such cells. This point is illustrated quantitatively using results from our simulations. At the low B cell affinity of $-14.8\ k_BT$, successful extraction of homotrimers in the cocktail frequently results from high forces on antigen-FDC bonds (Figure 2C), enabled by clustering of antigens and BCRs. When multiple BCRs pull on the same antigen, the force on the antigen-FDC bond is greater than the force on each of the antigen-BCR bonds (Figure 2A), so the off-rate of the former is relatively increased. The maximum possible force of 24 pN is realized when three BCRs are bound to one antigen, each contributing 8 pN of force. Using Equation 8, the off-rate for the antigen-FDC bond increases by ~300-fold when an antigen is bound by three BCRs, while the off-rate for each antigen-BCR bond increases by ~7-fold. For the strain-specific B cells capturing the chimera, however, the force on the antigen-FDC bond is always equal to the force on a single antigen-BCR bond because only one BCR can bind to an antigen (Figure 2A). Thus, the pulling forces do not increase the relative off-rate of the antigen-FDC bond compared with the antigen-BCR bonds. This is why low-affinity strain-specific B cells internalize smaller amounts of the heterotrimeric antigen than homotrimeric antigen (Figure 2B). For both types of immunogens, cross-reactive RBS-directed B cells can bind an antigen molecule with multiple BCRs (Figures 1F and S1B). So, at low affinity, these cells capture a larger amount of antigen relative to strain-specific B cells for the chimera and a similar amount of antigen for the cocktail (Figure 2B).

For high BCR affinity, the cross-reactive B cells capture more antigen than the strain-specific B cells do when interacting with the cocktail of homotrimers (Figure 2B). Beyond a certain affinity, the amount of antigen captured plateaus for the cocktail; this plateau corresponds to the B cell binding affinity approaching the antigen-FDC bond energy of $-19\ k_BT$. As a result, B cells capture most of the cognate antigens they encounter (Figure 2B). Consequently, antigen availability becomes a limiting factor, and cross-reactive B cells are favored because they can bind all antigens, while strain-specific B cells only recognize about a third of the antigen molecules presented in the cocktail. For the chimera, however, all antigen molecules can be internalized successfully even with monomeric bonds at very high affinity, so the advantage of cross-reactive B cells is small.

The results of antigen capture shown were obtained from simulations with 120 BCRs and 120 antigen molecules in the immune synapse. The multivalent antigen-BCR clustering behaviors are well manifested at this number (Figure S1B). Changing these numbers does not change the qualitative trends of antigen capture (Figures S1C and S1D) because they are the results of qualitative differences in the ways B cells and antigens engage based on their types, as described above.

Cross-reactive B cells evolve more readily upon immunization with the chimera when T cell help is a stringent constraint for positive selection of GC B cells

After antigen capture, B cells compete for positive selection by helper T cells by presenting the T cell epitopes that are derived from the internalized antigen. The homotrimeric cocktail allows only cross-reactive B cells to capture diverse rsHA components, while the nature of the chimeric design allows cross-reactive and strain-specific B cells to internalize all three components (Figure 3A). Thus, after immunization with the chimera, all B cells will compete for diverse T cells, and the differences in competitive advantages will be based on the amounts of antigen captured. However, if the T cell epitopes contained in each rsHA variant are distinct sets, then, upon immunization with the cocktail, only the cross-reactive B cells can interact with diverse T cells, while strain-specific B cells can only interact with a subset of the T cells (Figure 3A). This is because each T cell is specific for its epitope, and a single mutation within a TCR epitope or flanking sites can abrogate recognition.[54–57]

The rsHA components use antigenically distinct scaffolds derived from different subtypes, which results in large antigenic distances between the overall proteins (except for the RBS epitope). The large antigenic distance between the scaffolds raises the possibility that the components in the cocktail carry distinct T cell epitopes.

We used the Immune Epitope Database and Analysis Resource (IEDB) MHC class II binding prediction tool to analyze the predicted T cell epitopes in the H3, H4, and H14 rsHA components (Table S1).[58–62] Mice immunized with the cocktail or the chimera immunogens were mixed 129/Sv and C57BL/6 mice. Therefore, we used the I-A^b MHC allele to determine whether the T cell epitopes contained in the three HA components were distinct. None of the predicted 15-mer peptides that ranked in the top 20 percentile against randomly generated peptides were fully conserved in two different variants. When we relaxed the comparison criteria to just the 9-mer cores, still only two pairs were conserved in two different variants (Figure 3B). We further focused on the identity of just the amino acids at position 2 (P2), P5, P7, and P8 of the cores, which are the most likely T cell receptor (TCR)-contacting residues for the I-A^b haplotype.[63] Still, only five pairs were conserved in all pairwise comparisons (Figure 3C). In mice with the I-A^b haplotype, B cells that capture rabbit serum albumin and human serum albumin (76% sequence homology) do not compete with each other because of mutations in T cell epitopes.[64] For this rabbit and human serum albumin, we found 3 pairs of conserved 9-mer cores and 3 pairs of conserved P2, P5, P7, and P8 in both proteins, which is comparable with the resurfaced HA components (Figure S2). Therefore, we conclude that the components of the cocktail likely contain distinct T cell epitopes. We account for this feature in our simulations by keeping track of which antigens a B cell internalizes and partitioning helper T cells into three distinct groups based on their specificity for epitopes derived from each of the rsHA components. The number of T cells in each group is the same.

T cells make numerous short contacts with diverse B cells.[65] For each contact, there is a small chance of it being a productive encounter, which increases with the amount of peptide

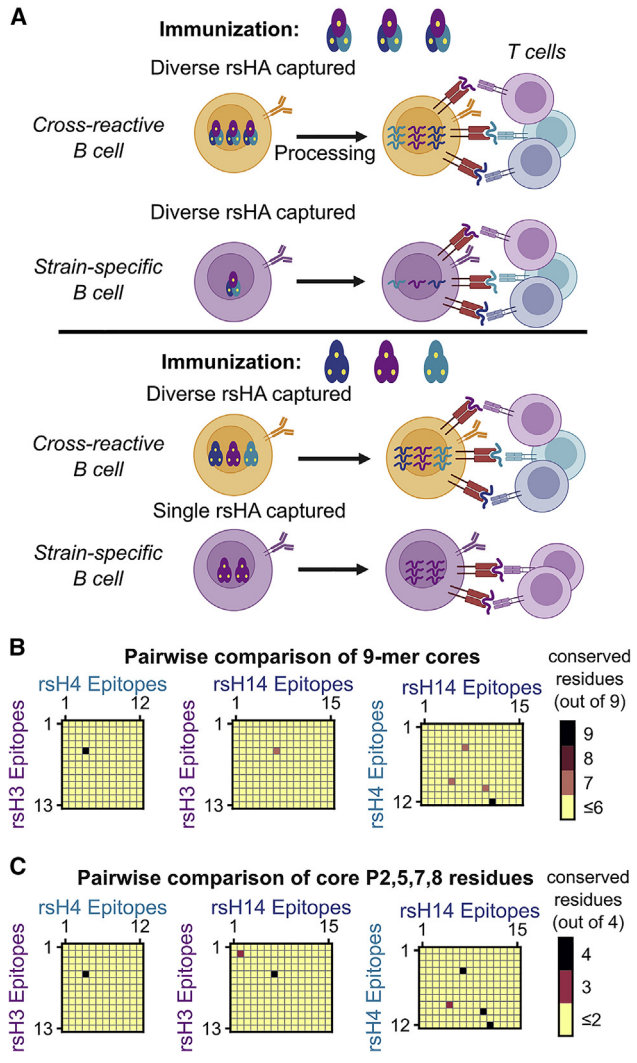

Figure 3. Effect of immunogen design on selection by T cells

(A) Schematics showing the differences between how cross-reactive and strain-specific B cells interact with helper T cells. For immunization with the chimera, strain-specific and cross-reactive B cells present pMHCs from all three rsHA components, but the cross-reactive B cells capture much more antigen. For the cocktail immunization, only the cross-reactive RBS-directed B cells present pMHCs derived from multiple rsHA components, but the amount of antigen captured is not sufficiently different.

(B and C) Pairwise comparison of computationally predicted helper T cell epitopes in the rsHA components. Each axis corresponds to the ranks of the top 20th percentile predicted 15-mer T cell epitopes, derived from the three rsHA components.

(B) Number of conserved residues in pairwise comparisons of the 9-mer cores of the predicted epitopes.

(C) Number of conserved residues in pairwise comparisons of the P2, P5, P7, and P8 residues of the 9-mer cores.

See also Table S1 and Figure S2.

presented.[66] It is conjectured that positive selection likely requires several productive encounters.[67] Therefore, the amount of help a B cell receives will increase with the number of encounters with cognate T cells, which is determined by the types of pMHC it presents, the number of cognate T cells, and the number of competing B cells. Therefore, we represent the probability of positive selection of a B cell i as follows:

$$P_i = P_{max}\frac{\sum_k \left(\frac{T_k}{N_{B,k}}\right)\cdot\left(\frac{A_{ki}}{\langle A_k\rangle}\right)^{\chi}}{1+\sum_k \left(\frac{T_k}{N_{B,k}}\right)\cdot\left(\frac{A_{ki}}{\langle A_k\rangle}\right)^{\chi}} \quad \text{(Equation 9)}$$

where A_{ki} is the amount of the HA component k internalized by the B cell i, $\langle A_k\rangle$ is the mean amount of HA component k internalized by the B cells that recognize this component, $N_{B,k}$ is the number of such B cells, and T_k is the number of T cells that target the epitopes from the HA component k, which we assume to be equal for all variants. The maximum probability of selection, P_{max}, accounts for the fact that GC B cells are inherently apoptotic irrespective of BCR affinity.[68] We can consider P_{max} to be the chance of avoiding the default fate of apoptosis: $1-P_{apoptosis}$. We chose $P_{max}=0.6$ because it results in good correspondence between the timescales of our model results and experiments; other values were also tested, and the qualitative result does not change.

An important feature of the model is the exponent χ; larger values of it imply that T cell help depends more stringently on the amount of pMHC presented. If χ is less than 1, then small differences (e.g., 2-fold) in pMHC displayed on two B cells would have a relatively small effect on selection outcome, whereas if χ is greater than 1, then such small differences would likely lead to selection of the B cell that displays more pMHC.

Figure 4A shows predictions of our model upon immunization with the chimeric and cocktail immunogens for the temporal evolution of the fraction of GC B cells that evolve from the initial RBS-directed B cell precursors; i.e., B cells that have acquired higher binding affinities than the precursors. A striking feature of these results is that, for immunization with the chimera immunogen, the evolution of RBS-directed B cells becomes increasingly more efficient as T cell selection becomes more stringent (larger values of χ), but for immunization with the cocktail immunogen, the opposite is true. Figure 4B shows the fraction of evolved RBS-directed B cells that are cross reactive toward at least two rsHA components in the immunogens. A low value indicates that RBS-directed B cells tend to specialize to only one component. Our model predicts that cross-reactive mutants evolve more readily upon immunization with the cocktail when T cell help is permissive but with the chimera when T cell help is stringent. The cocktail improves in selecting cross-reactive B cells in the late GC when T cell help is stringent because of the advantages in antigen capture at high affinity (Figure 2B). However, by day 14, only a small fraction (12% for $x=1.5$) of the simulated GCs still have any RBS-directed B cell (Figure S3A). So, our model predicts that cross-reactive RBS-directed B cells will evolve more readily upon immunization with the chimera compared with the cocktail when T cell help is a stringent constraint for positive selection of B cells. Figures S3B and S3C show that this qualitative trend is not changed when ρ is changed to 0.4 or when P_{max} is changed to 1.

In Figure 4C, we compare the model predictions with the experimental findings by Caradonna et al.[35] for the fraction of B cells that are RBS directed and cross reactive in early and

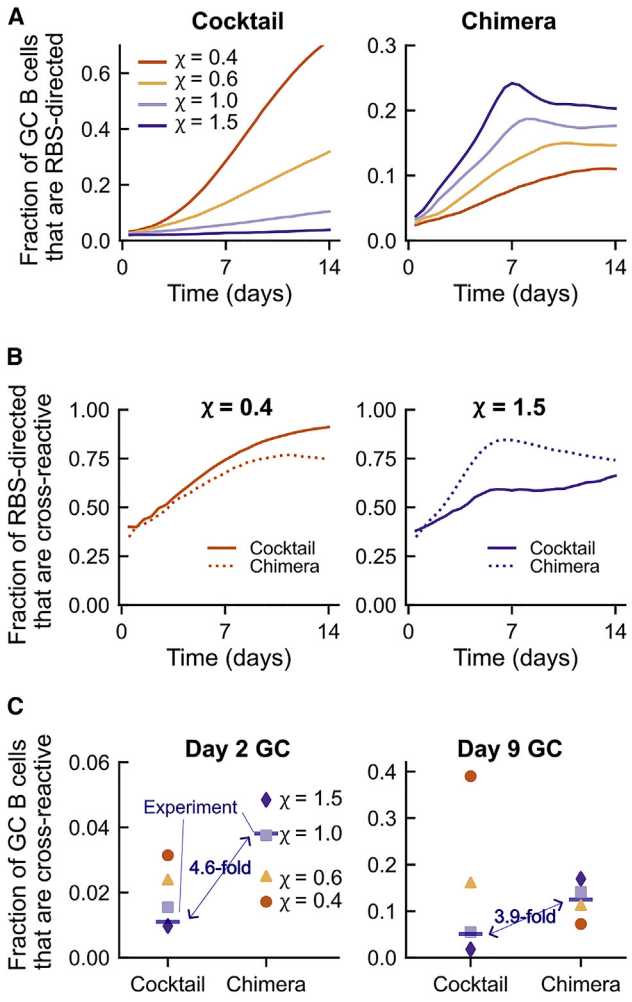

Figure 4. Model predictions and experimental results for the expansion and evolution of cross-reactive B cells upon immunization with the cocktail or the chimera immunogen

(A) Fraction of GC B cells that are RBS directed as a function of time in the simulations. Changing the stringency of T cell selection has opposite effects for immunization with the chimera or the cocktail immunogen.

(B) Fraction of RBS-directed B cells that are cross reactive. When selection by T cells is permissive ($\chi < 1$), the cocktail outperforms the chimera for evolving cross-reactive B cells. The opposite is true for stringent selection ($\chi \geq 1$).

(C) Fraction of GC B cells that are RBS directed and cross reactive in early and late GCs. Model predictions for varying levels of T cell selection stringency are compared with the results of mouse immunization experiments. All fractions were calculated after combining B cells from 1,000 independent stochastic simulations.

See also Figure S3.

late GCs after immunization with either type of immunogen. These data represent the combined objectives of expanding rare RBS-directed B cells (Figure 4A) and shepherding them to accumulate cross-reactive mutations (Figure 4B). We assume that days 8 and 15 post immunization in experiments correspond to days 2 and 9 of the GC because GC initiation typically takes about 6 days.[69] While Caradonna et al.[35] report the value as a fraction of all immunoglobulin G $(IgG)^+$ GC B cells, because our model does not consider background GC B cells that do not bind to any rsHA, we only consider the B cells that bind to at least one rsHA component from the experimental data. The qualitative trends in the data are not affected by the background B cells.

The experiments show a qualitatively higher frequency of cross-reactive RBS-directed B cells in GCs on day 8 and day 15 after immunization with the chimera.[35] These experimental results are consistent with our predictions when T cell help is stringent but not when it is permissive. The model predicts that, if T cell help is stringent ($\chi \geq 1$), a higher fraction of GC B cells will be RBS directed and cross reactive after immunization with the chimera than with the cocktail (Figure 4C). If $\chi = 1$, then 3.8% of B cells in day 2 GCs are RBS directed and cross reactive after chimera immunization and 1.5% after the cocktail immunization. On day 9, the numbers are 14% for the chimera and 5.5% for the cocktail. In contrast, if T cell help is permissive ($\chi < 1$), then the cocktail favors the evolution of cross-reactive B cells. For example, if $\chi = 0.4$, then 3.1% of B cells in day 2 GCs are RBS directed and cross reactive after cocktail immunization and 1.7% after the chimera immunization; the same trend is true on day 9 (39% for the cocktail and 7.2% for the chimera). We emphasize that what is important is not the precise numbers noted above but that the qualitative trend of which type of immunogen promotes the evolution of RBS-directed cross-reactive antibodies is opposite for stringent versus permissive selection by helper T cells. The model predictions have the same trend as the experimental data when T cell help is a stringent constraint. Therefore, we conclude that T cell help stringently depends on pMHC density. We also note that, even under the most stringent selection tested ($\chi = 1.5$), stochasticity in evolution allows clonal heterogeneities inside individual GCs (Figure S3D)[41] and broad affinity distribution of B cells within and across GCs (Figure S3E),[40] consistent with previous findings in the literature.

Mechanism for why T cell selection stringency promotes cross-reactive B cell evolution for the chimera immunogen but not the cocktail

Events that occur in the early GC are critically important for the RBS-directed precursors because they are few in number and could be easily extinguished because of stochastic effects. For the chimera immunogen, cross-reactive RBS-directed B cells can bind to the antigen multivalently while strain-specific B cells cannot, so the former can capture significantly more antigen than the latter in the early stages of the GC reaction (Figure 2). Thus, to promote the evolution of RBS-directed B cells, their principal advantage over off-target B cells (more antigen captured) must be amplified by the selection force. This advantage is amplified when positive selection by helper T cells discriminates stringently based on the amount of captured antigen because this favors selection of the cross-reactive B cells. Indeed, our simulation results show that the probability that RBS-directed precursors are positively selected in the early GC grows with the value of χ upon immunization with the chimera (Figure 5A). If RBS-directed B cells are more readily positively selected in the early GC, then they multiply more and thus have a higher chance of acquiring the rare mutations that confer breadth. Such an effect of an early advantage affecting future fate has been observed in evolving asexual populations.[70] Consistent with this expectation, simulation results under

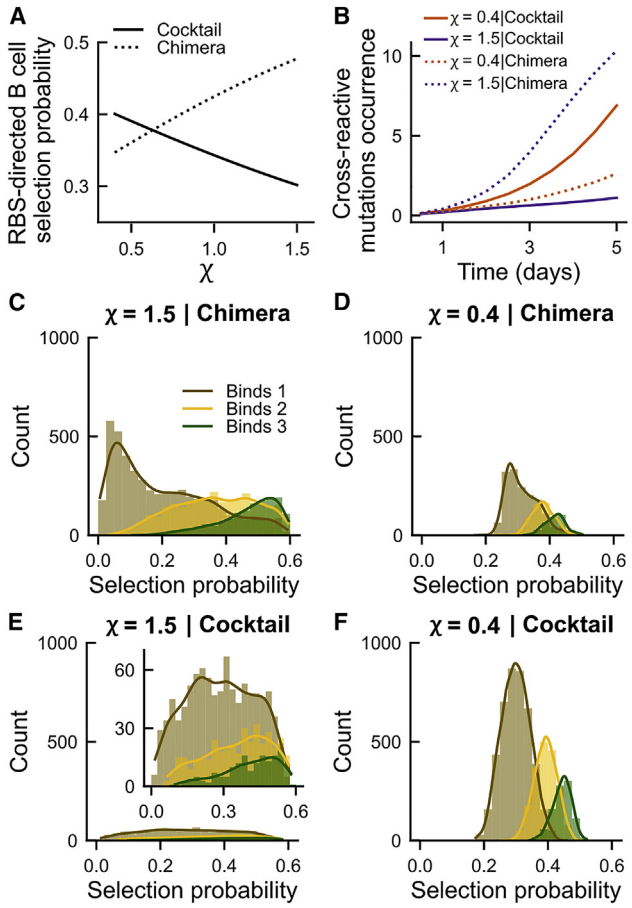

Figure 5. Potential mechanism of how T cell selection stringency affects expansion and evolution of RBS-directed B cells

(A) Selection probability of the RBS-directed B cell precursor at GC initiation as a function of T cell help stringency.

(B) Average number of unique mutations that occur in a GC in the first 5 days that increase the affinities of RBS-directed B cells toward multiple rsHA components.

(A and B) The effects of T cell selection stringency are opposite for immunizations with the cocktail and chimera.

(C–F) Positive selection probabilities of unique RBS-directed B cell mutants in day 5 GCs, simulated under either stringent T cell selection (C and E) or permissive T cell selection (D and F) conditions after immunization with either the chimera (C and D) or the cocktail (E and F). The mutants are classified based on how many rsHA components they can bind (from one to three).

stringent T cell selection show that, upon immunization with the chimera, rare mutations that confer breadth are quickly found in the population (Figure 5B). The resulting cross-reactive cells are then selected for and proliferate because they have a large advantage in antigen capture, which translates to a high probability of selection by T cells (Figure 5C).

Specializing mutations occur frequently for RBS-directed B cells, but such mutations result in loss of cross-reactivity, and this inhibits antigen capture. When selection is stringent, this disadvantage in the amount of antigen captured is magnified during selection. In early GCs (day 5), when selection is stringent ($\chi = 1.5$), the median selection probability of the RBS-directed B cells that bind all three rsHA components and that of the B cells that bind only one is 0.49 and 0.17, respectively (Figure 5C). When selection is permissive ($\chi = 0.4$), the corresponding values are 0.40 and 0.30 (Figure 5D). Therefore, while mutations generate strain-specific RBS-directed B cells in both cases, these mutated B cells are more heavily disfavored when selection is stringent. These reasons promote cross-reactive B cell evolution upon immunization with the chimera when T cell selection is a stringent constraint.

For immunization with the cocktail immunogens, the difference in the amounts of antigen captured by low-affinity, cross-reactive, and strain-specific B cells is small in the early GC when antigen is not limiting (Figure 2B). Therefore, increasing the stringency of how positive selection probability depends on the amount of antigen captured will not favor the cross-reactive B cells. The predominant difference between the cross-reactive and strain-specific B cells in the early GC is that only the former can capture diverse types of rsHA components so it can be positively selected by T cells with diverse epitope specificities, while the latter seeks help from only a part of the repertoire of helper T cells. Cross-reactive B cells are promoted when this difference helps them during T cell selection. If selection stringency is permissive, then each encounter with a cognate helper T cell will give a similar chance of receiving positive selection signals. Cross-reactive B cells will encounter cognate T cells more frequently by capturing diverse epitopes, and despite the lower pMHC density of each epitope, the total probability of receiving help will be greater than strain-specific B cells that capture a similar total amount of antigen. Mathematical analysis of Equation 9 (STAR Methods) shows that this is true when $\chi < 1$. Consistent with this analysis, our simulation results show that the selection probability of RBS-directed precursors in the early GC increases with decreasing χ (Figure 5A). The enhanced early selection probability allows RBS-directed B cells to more readily evolve future cross-reactive mutations (Figure 5B). The cross-reactive mutants have a distinct advantage over strain-specific mutants when selection is permissive and therefore selectively accumulate, but not when selection is stringent (Figures 5E and 5F). This is because, for less stringent selection, the ability of cross-reactive B cells to be positively selected by interacting with diverse T cells is amplified.

DISCUSSION

Eliciting bnAbs is a necessary step toward a universal influenza vaccine that confers protection against seasonal variants and pandemic-causing novel strains. Influenza RBS is a promising target for bnAbs, but germline B cell precursors that target the RBS are rare relative to off-target sites,[32] and affinity-matured RBS-directed B cells often have low breadth because they strongly interact with the variable residues within their footprints.[37,71] Thus, vaccination strategies to amplify the rare RBS-directed B cell precursors and shepherd their mutation pathways toward high breadth are required. Here, we study the evolution of cross-reactive B cells that target the conserved HA RBS upon immunization with either a heterotrimeric RBS-enriched chimera or a cocktail of three homotrimeric rsHAs.[35] Toward this end, we developed a computational model of affinity maturation upon vaccination with the chimera and cocktail

immunogens. Our analyses of the pertinent processes and simulation results (Figures 1–5) provide mechanistic insights into the factors that influence antibody repertoire development upon vaccination with different types of immunogens.

We identify two important variables: the valency with which the antigen is bound to BCR and the diversity of antigens captured by B cells. If cross-reactive B cells engage antigen multivalently and strain-specific B cells cannot, as is true for the chimera (Figure 2), then stringent selection of GC B cells by helper T cells promotes cross-reactive B cell evolution (Figures 4 and 5). If the diversity of antigens captured is the principal difference between cross-reactive and strain-specific B cells, as is true for the cocktail (Figures 2 and 3), then selection stringency must be permissive to promote the evolution of cross-reactive B cells (Figures 4 and 5). Because cross-reactive B cells are more enriched in mice immunized with the chimera immunogen, we conclude that positive selection of B cells by helper T cells is a stringent constraint during GC reactions. Thus, our studies provide fundamental mechanistic insights into the role of T cell help during affinity maturation,[39–41,43,72] which will help improve vaccine design.

Our result suggests that one promising future direction would be to further optimize antigen valency using nanoparticles and epitope enrichment to maximize the difference between the antigen capture capabilities of cross-reactive and strain-specific B cells. Furthermore, we show that stringent selection by T cells will maximize the efficacy of such immunogens. Many nanoparticle-based immunogens that aim to optimize antigen capture by cross-reactive B cells have large non-native protein cores,[13,73–75] which can contain many highly immunogenic helper T cell epitopes.[76] However, an understanding of how this addition might affect selection by helper T cells and the efficacy of the designed immunogens is currently lacking. Our study highlights the need for a better understanding of this relationship.

Alternatively, our model predicts that if T cell selection is permissive, then a cocktail of antigens with distinct T cell epitopes can be highly effective at eliciting cross-reactive B cells. There is evidence that some T follicular helper cells are of higher "quality" than others; that is, they can maintain a greater GC B cell/T follicular helper cell ratio.[77,78] This observation suggests that such helper T cells may have more frequent productive encounters with B cells while being less stringent regarding the amounts of pMHC presented by the B cells, consistent with permissive selection in our model. This hypothesis can be tested by combining adoptive transfer of T cells and graded delivery of peptides to GC B cells.[38] Alternatively, it has been suggested that upregulating key surface adhesion molecules on T cells, such as signalling lymphocytic activation molecule (SLAM) and SLAM-associated protein (SAP), may make them more potent helpers.[79] Upregulation of adhesion molecules in dendritic cells and macrophages enhanced their abilities to activate adaptive immune cells,[80] and a similar approach could be applied to T cells to study its effect on selection stringency. Finally, we can ask whether increasing the total number of T cells affects the stringency of selection by individual T cells, which can be tested by adoptive transfer of different numbers of T cells. The answer will depend on the mechanisms of selection by the T cells. Testing these hypotheses to further improve our computational model and immunogen designs will shed light on basic questions in immunology and vaccine design.

Our results are generalizable for other epitope targets: first, when amplification of rare B cells that target a conserved epitope is the goal, and second, when a selective accumulation of mutations that confer high breadth is needed. However, it will also be necessary to consider the constraints of the specific target. For example, for HIV CD4 binding site bnAbs, germline-targeting immunogens are usually first used to amplify the rare germline precursors.[81] The approaches presented in this study can be applied for shepherding the mutations required for these precursor B cells to evolve into bnAbs. This is because strain-specific variable residues shield the CD4 binding site, making the exposed conserved target smaller than typical BCR footprints.[34] For the stem epitope of influenza, the shepherding step may not be as important because the conserved region is large.[82] However, the steric hindrance for B cells to bind to this target is also a critical consideration for an effective immunogen design.[83] Thus, an interesting future direction may be to study how the design principles outlined by our study can be incorporated with other design constraints specific to various targets of bnAbs.

Limitations of the study

We used a coarse-grained representation of the immune response to limit the number of uncertain parameters in the model and derive key mechanistic insights. For example, we used a simplified mathematical representation of selection by helper T cells, which allowed us to highlight the importance of the stringency of selection and shed light on this issue. However, while our model of antigen capture and T cell help explains the experimental observations, we have not directly proven the suggested mechanism. Further experiments based on our findings will be necessary to provide definitive proof.

STAR★METHODS

Detailed methods are provided in the online version of this paper and include the following:

- KEY RESOURCES TABLE
- RESOURCE AVAILABILITY
  - Lead contact
  - Materials availability
  - Data and code availability
- METHOD DETAILS
  - Affinity maturation simulation algorithm
  - Simulation of antigen capture
  - Selection by T cells
  - T cell epitope prediction and comparison
- QUANTIFICATION AND STATISTICAL ANALYSIS

SUPPLEMENTAL INFORMATION

Supplemental information can be found online at https://doi.org/10.1016/j.celrep.2023.112160.

ACKNOWLEDGMENTS

We thank Dr. Assaf Amitai for helpful discussions and critical insights. L.Y. and A.K.C. were supported by NIH grant U19AI057229 and funds from the Ragon Institute, and we acknowledge support from the NIH for R01AI146779 (to

A.G.S.), P01AI89618-A1 (to A.G.S.), and T32 GM007753 (to T.M.C.). Work for this manuscript has been funded in whole or part by federal funds under a contract from the National Institute of Allergy and Infectious Diseases, NIH contract 75N93019C00050 (to A.G.S.) L.Y. also acknowledges partial funding from the Kwanjeong Educational Foundation. The BioRender software was used for parts of Figures 1–4 and Figure S1.

AUTHOR CONTRIBUTIONS

L.Y., T.M.C., A.K.C., and A.G.S. designed the research. L.Y. carried out the calculations. A.K.C. and L.Y. analyzed the data. A.K.C., L.Y., T.M.C., and A.G.S. connected the experimental and computational results and wrote the paper.

DECLARATION OF INTERESTS

A.K.C. is a consultant (titled Academic Partner) for Flagship Pioneering and also serves on the Strategic Oversight Board of its affiliated company, Apriori Bio, and is a consultant and SAB member of another affiliated company, FL72.

INCLUSION AND DIVERSITY

One or more of the authors of this paper self-identifies as a member of the LGBTQIA+ community.

Received: February 15, 2022
Revised: July 18, 2022
Accepted: February 9, 2023
Published: March 2, 2023

REFERENCES

1. Zhou, D., Dejnirattisai, W., Supasa, P., Liu, C., Mentzer, A.J., Ginn, H.M., Zhao, Y., Duyvesteyn, H.M.E., Tuekprakhon, A., Nutalai, R., et al. (2021). Evidence of escape of SARS-CoV-2 variant B.1.351 from natural and vaccine-induced sera. Cell *184*, 2348–2361.e6. https://doi.org/10.1016/j.cell.2021.02.037.
2. Cao, Y., Wang, J., Jian, F., Xiao, T., Song, W., Yisimayi, A., Huang, W., Li, Q., Wang, P., An, R., et al. (2022). Omicron escapes the majority of existing SARS-CoV-2 neutralizing antibodies. Nature *602*, 657–663. https://doi.org/10.1038/s41586-021-04385-3.
3. Hraber, P., Seaman, M.S., Bailer, R.T., Mascola, J.R., Montefiori, D.C., and Korber, B.T. (2014). Prevalence of broadly neutralizing antibody responses during chronic HIV-1 infection. AIDS *28*, 163–169. https://doi.org/10.1097/QAD.0000000000000106.
4. Simek, M.D., Rida, W., Priddy, F.H., Pung, P., Carrow, E., Laufer, D.S., Lehrman, J.K., Boaz, M., Tarragona-fiol, T., Miiro, G., et al. (2009). Human immunodeficiency virus type 1 elite neutralizers: individuals with broad and potent neutralizing activity identified by using a high-throughput neutralization assay together with an analytical selection algorithm. J. Virol. *83*, 7337–7348. https://doi.org/10.1128/JVI.00110-09.
5. Burton, D.R., Pyati, J., Koduri, R., Sharp, S.J., Thornton, G.B., Parren, P.W., Sawyer, L.S., Hendry, R.M., Dunlop, N., Nara, P.L., et al. (1994). Efficient neutralization of primary isolates of HIV-1 by a recombinant human monoclonal antibody. Science *266*, 1024–1027. https://doi.org/10.1126/science.7973652.
6. Corti, D., Suguitan, A.L., Pinna, D., Silacci, C., Fernandez-Rodriguez, B.M., Vanzetta, F., Santos, C., Luke, C.J., Torres-Velez, F.J., Temperton, N.J., et al. (2010). Heterosubtypic neutralizing antibodies are produced by individuals immunized with a seasonal influenza vaccine. J. Clin. Invest. *120*, 1663–1673. https://doi.org/10.1172/JCI41902.
7. Wrammert, J., Koutsonanos, D., Li, G.M., Edupuganti, S., Sui, J., Morrissey, M., Mccausland, M., Skountzou, I., Hornig, M., Lipkin, W.I., et al. (2011). Broadly cross-reactive antibodies dominate the human B cell response against 2009 pandemic H1N1 influenza virus infection. J. Exp. Med. *208*, 181–193. https://doi.org/10.1084/jem.20101352.
8. Whittle, J.R.R., Zhang, R., Khurana, S., King, L.R., Manischewitz, J., Golding, H., Dormitzer, P.R., Haynes, B.F., Walter, E.B., Moody, M.A., et al. (2011). Broadly neutralizing human antibody that recognizes the receptor-binding pocket of influenza virus hemagglutinin. Proc. Natl. Acad. Sci. USA *108*, 14216–14221. https://doi.org/10.1073/pnas.1111497108.
9. Stamatatos, L., Morris, L., Burton, D.R., and Mascola, J.R. (2009). Neutralizing antibodies generated during natural hiv-1 infection: good news for an hiv-1 vaccine? Nat. Med. *15*, 866–870. https://doi.org/10.1038/nm.1949.
10. Sui, J., Sheehan, J., Hwang, W.C., Bankston, L.A., Burchett, S.K., Huang, C.Y., Liddington, R.C., Beigel, J.H., and Marasco, W.A. (2011). Wide prevalence of heterosubtypic broadly neutralizing human anti-influenza a antibodies. Clin. Infect. Dis. *52*, 1003–1009. https://doi.org/10.1093/cid/cir121.
11. Jardine, J.G., Ota, T., Sok, D., Pauthner, M., Kulp, D.W., Kalyuzhniy, O., Skog, P.D., Thinnes, T.C., Bhullar, D., Briney, B., et al. (2015). Priming a broadly neutralizing antibody response to HIV-1 using a germline-targeting immunogen. Science *349*, 156–161. https://doi.org/10.1126/science.aac5894.
12. Steichen, J.M., Lin, Y.C., Havenar-Daughton, C., Pecetta, S., Ozorowski, G., Willis, J.R., Toy, L., Sok, D., Liguori, A., Kratochvil, S., et al. (2019). A generalized HIV vaccine design strategy for priming of broadly neutralizing antibody responses. Science *366*, eaax4380. https://doi.org/10.1126/science.aax4380.
13. Kanekiyo, M., Joyce, M.G., Gillespie, R.A., Gallagher, J.R., Andrews, S.F., Yassine, H.M., Wheatley, A.K., Fisher, B.E., Ambrozak, D.R., Creanga, A., et al. (2019). Mosaic nanoparticle display of diverse influenza virus hemagglutinins elicits broad B cell responses. Nat. Immunol. *20*, 362–372. https://doi.org/10.1038/s41590-018-0305-x.
14. Escolano, A., Steichen, J.M., Dosenovic, P., Kulp, D.W., Golijanin, J., Sok, D., Freund, N.T., Gitlin, A.D., Oliveira, T., Araki, T., et al. (2016). Sequential immunization elicits broadly neutralizing anti-HIV-1 antibodies in Ig knockin mice. Cell *166*, 1445–1458.e12. https://doi.org/10.1016/j.cell.2016.07.030.
15. Torrents de la Peña, A., de Taeye, S.W., Sliepen, K., LaBranche, C.C., Burger, J.A., Schermer, E.E., Montefiori, D.C., Moore, J.P., Klasse, P.J., and Sanders, R.W. (2018). Immunogenicity in rabbits of HIV-1 SOSIP trimers from clades A, B, and C, given individually, sequentially, or in combination. J. Virol. *92*, e01957019577-17. https://doi.org/10.1128/jvi.01957-17.
16. Wang, S., Mata-Fink, J., Kriegsman, B., Hanson, M., Irvine, D.J., Eisen, H.N., Burton, D.R., Wittrup, K.D., Kardar, M., and Chakraborty, A.K. (2015). Manipulating the selection forces during affinity maturation to generate cross-reactive HIV antibodies. Cell *160*, 785–797. https://doi.org/10.1016/j.cell.2015.01.027.
17. Shaffer, J.S., Moore, P.L., Kardar, M., and Chakraborty, A.K. (2016). Optimal immunization cocktails can promote induction of broadly neutralizing Abs against highly mutable pathogens. Proc. Natl. Acad. Sci. USA *113*, E7039–E7048. https://doi.org/10.1073/pnas.1614940113.
18. Sprenger, K.G., Louveau, J.E., Murugan, P.M., and Chakraborty, A.K. (2020). Optimizing immunization protocols to elicit broadly neutralizing antibodies. Proc. Natl. Acad. Sci. USA *117*, 20077–20087. https://doi.org/10.1073/PNAS.1919329117.
19. Meyer-Hermann, M. (2019). Injection of antibodies against immunodominant epitopes tunes germinal centers to generate broadly neutralizing antibodies. Cell Rep. *29*, 1066–1073.e5. https://doi.org/10.1016/j.celrep.2019.09.058.
20. Childs, L.M., Baskerville, E.B., and Cobey, S. (2015). Trade-offs in antibody repertoires to complex antigens. Philos. Trans. R. Soc. Lond. B Biol. Sci. *370*, 20140245. https://doi.org/10.1098/rstb.2014.0245.
21. Murugan, R., Buchauer, L., Triller, G., Kreschel, C., Costa, G., Pidelaserra Martí, G., Imkeller, K., Busse, C.E., Chakravarty, S., Sim, B.K.L., et al. (2018). Clonal selection drives protective memory B cell responses in controlled human malaria infection. Sci. Immunol. *3*, eaap8029. https://doi.org/10.1126/sciimmunol.aap8029.

22. Luo, S., and Perelson, A.S. (2015). Competitive exclusion by autologous antibodies can prevent broad HIV-1 antibodies from arising. Proc. Natl. Acad. Sci. USA *112*, 11654–11659. https://doi.org/10.1073/pnas.1505207112.

23. Ganti, R.S., and Chakraborty, A.K. (2021). Mechanisms underlying vaccination protocols that may optimally elicit broadly neutralizing antibodies against highly mutable pathogens. Phys. Rev. E *103*, 052408. https://doi.org/10.1103/physreve.103.052408.

24. Sachdeva, V., Husain, K., Sheng, J., Wang, S., and Murugan, A. (2020). Tuning environmental timescales to evolve and maintain generalists. Proc. Natl. Acad. Sci. USA *117*, 12693–12699. https://doi.org/10.1073/pnas.1914586117.

25. de Boer, R.J., and Perelson, A.S. (2017). How germinal centers evolve broadly neutralizing antibodies: the breadth of the follicular helper T cell response. J. Virol. *91*, 1009833-17.

26. Nourmohammad, A., Otwinowski, J., and Plotkin, J.B. (2016). Host-pathogen coevolution and the emergence of broadly neutralizing antibodies in chronic infections. PLoS Genet. *12*, e1006171. https://doi.org/10.1371/journal.pgen.1006171.

27. Victora, G.D., and Nussenzweig, M.C. (2012). Germinal centers. Annu. Rev. Immunol. *30*, 429–457. https://doi.org/10.1146/annurev-immunol-020711-075032.

28. Nowosad, C.R., Spillane, K.M., and Tolar, P. (2016). Germinal center B cells recognize antigen through a specialized immune synapse architecture. Nat. Immunol. *17*, 870–877. https://doi.org/10.1038/ni.3458.

29. Victora, G.D., Schwickert, T.A., Fooksman, D.R., Kamphorst, A.O., Meyer-Hermann, M., Dustin, M.L., and Nussenzweig, M.C. (2010). Germinal center dynamics revealed by multiphoton microscopy with a photoactivatable fluorescent reporter. Cell *143*, 592–605. https://doi.org/10.1016/j.cell.2010.10.032.

30. Jardine, J.G., Kulp, D.W., Havenar-Daughton, C., Sarkar, A., Briney, B., Sok, D., Sesterhenn, F., Ereño-Orbea, J., Kalyuzhniy, O., Deresa, I., et al. (2016). HIV-1 broadly neutralizing antibody precursor B cells revealed by germline-targeting immunogen. Science *351*, 1458. https://doi.org/10.1126/science.aad9195.

31. Pantophlet, R., Wilson, I.A., and Burton, D.R. (2003). Hyperglycosylated mutants of human immunodeficiency virus (HIV) type 1 monomeric gp120 as novel antigens for HIV vaccine design. J. Virol. *77*, 5889–5901. https://doi.org/10.1128/jvi.77.10.5889-5901.2003.

32. Schmidt, A.G., Therkelsen, M.D., Stewart, S., Kepler, T.B., Liao, H.X., Moody, M.A., Haynes, B.F., and Harrison, S.C. (2015). Viral receptor-binding site antibodies with diverse germline origins. Cell *161*, 1026–1034. https://doi.org/10.1016/j.cell.2015.04.028.

33. Wu, N.C., Grande, G., Turner, H.L., Ward, A.B., Xie, J., Lerner, R.A., and Wilson, I.A. (2017). In vitro evolution of an influenza broadly neutralizing antibody is modulated by hemagglutinin receptor specificity. Nat. Commun. *8*, 15371. https://doi.org/10.1038/ncomms15371.

34. Kwong, P.D., Doyle, M.L., Casper, D.J., Cicala, C., Leavitt, S.A., Majeed, S., Steenbeke, T.D., Venturi, M., Chaiken, I., Fung, M., et al. (2002). HIV-1 evades antibody-mediated neutralization through conformational masking of receptor-binding sites. Nature *420*, 678–682. https://doi.org/10.1038/nature01188.

35. Caradonna, T.M., Windsor, I.W., Roffler, A.A., Song, S., Watanabe, A., Kelsoe, G., Kuraoka, M., and Schmidt, A.G. (2022). An epitope-enriched immunogen increases site targeting in germinal centers. Preprint at bioRxiv. https://doi.org/10.1101/2022.12.01.518697.

36. Bajic, G., Maron, M.J., Caradonna, T.M., Tian, M., Mermelstein, A., Fera, D., Kelsoe, G., Kuraoka, M., and Schmidt, A.G. (2020). Structure-guided molecular grafting of a complex broadly neutralizing viral epitope. ACS Infect. Dis. *6*, 1182–1191. https://doi.org/10.1021/acsinfecdis.0c00008.

37. Caradonna, T.M., Ronsard, L., Yousif, A.S., Windsor, I.W., Hecht, R., Bracamonte-Moreno, T., Roffler, A.A., Maron, M.J., Maurer, D.P., Feldman, J., et al. (2022). An epitope-enriched immunogen expands responses to a conserved viral site. Cell Rep. *41*, 111628. https://doi.org/10.1016/J.CELREP.2022.111628.

38. Gitlin, A.D., Shulman, Z., and Nussenzweig, M.C. (2014). Clonal selection in the germinal centre by regulated proliferation and hypermutation. Nature *509*, 637–640. https://doi.org/10.1038/nature13300.

39. Yeh, C.H., Nojima, T., Kuraoka, M., and Kelsoe, G. (2018). Germinal center entry not selection of B cells is controlled by peptide-MHCII complex density. Nat. Commun. *9*, 928. https://doi.org/10.1038/s41467-018-03382-x.

40. Kuraoka, M., Schmidt, A.G., Nojima, T., Feng, F., Watanabe, A., Kitamura, D., Harrison, S.C., Kepler, T.B., and Kelsoe, G. (2016). Complex antigens drive permissive clonal selection in germinal centers. Immunity *44*, 542–552. https://doi.org/10.1016/j.immuni.2016.02.010.

41. Tas, J.M.J., Mesin, L., Pasqual, G., Targ, S., Jacobsen, J.T., Mano, Y.M., Chen, C.S., Weill, J.C., Reynaud, C.A., Browne, E.P., et al. (2016). Visualizing antibody affinity maturation in germinal centers. Science *351*, 1048–1054. https://doi.org/10.1126/science.aad3439.

42. Meyer-Hermann, M., Mohr, E., Pelletier, N., Zhang, Y., Victora, G.D., and Toellner, K.M. (2012). A theory of germinal center b cell selection, division, and exit. Cell Rep. *2*, 162–174. https://doi.org/10.1016/j.celrep.2012.05.010.

43. Mesin, L., Ersching, J., and Victora, G.D. (2016). Germinal center B cell dynamics. Immunity *45*, 471–482. https://doi.org/10.1016/j.immuni.2016.09.001.

44. Sablitzky, F., Wildner, G., and Rajewsky, K. (1985). Somatic mutation and clonal expansion of B cells in an antigen-driven immune response. EMBO J. *4*, 345–350. https://doi.org/10.1002/j.1460-2075.1985.tb03635.x.

45. Batista, F.D., and Neuberger, M.S. (1998). Affinity dependence of the B cell response to antigen: a threshold, a ceiling, and the importance of off-rate. Immunity *8*, 751–759. https://doi.org/10.1016/S1074-7613(00)80580-4.

46. Zhang, J., and Shakhnovich, E.I. (2010). Optimality of mutation and selection in germinal centers. PLoS Comput. Biol. *6*, e1000800. https://doi.org/10.1371/journal.pcbi.1000800.

47. Kumar, M.D.S., and Gromiha, M.M. (2006). Pint : protein – protein interactions thermodynamic database. Nucleic Acids Res. *34*, 195–198. https://doi.org/10.1093/nar/gkj017.

48. Natkanski, E., Lee, W.-Y., Mistry, B., Casal, A., Molloy, J.E., and Tolar, P. (2013). B cells use mechanical energy to discriminate antigen affinities. Science *340*, 1587–1590.

49. Tsourkas, P.K., Baumgarth, N., Simon, S.I., and Raychaudhuri, S. (2007). Mechanisms of B-cell synapse formation predicted by Monte Carlo simulation. Biophys. J. *92*, 4196–4208. https://doi.org/10.1529/biophysj.106.094995.

50. Fleire, S.J., Goldman, J.P., Carrasco, Y.R., Weber, M., Bray, D., and Batista, F.D. (2006). B cell ligand discrimination through a spreading and contraction response. Science *312*, 738–741. https://doi.org/10.1126/science.1123940.

51. Amitai, A., Chakraborty, A.K., and Kardar, M. (2018). The low spike density of HIV may have evolved because of the effects of T helper cell depletion on affinity maturation. PLoS Comput. Biol. *14*, e1006408. https://doi.org/10.1371/journal.pcbi.1006408.

52. Bell, G.I. (1978). Models for the specific adhesion of cells to cells. Science *200*, 618–627. https://doi.org/10.1126/science.347575.

53. Erdmann, T., and Schwarz, U.S. (2004). Stochastic dynamics of adhesion clusters under shared constant force and with rebinding. J. Chem. Phys. *121*, 8997–9017. https://doi.org/10.1063/1.1805496.

54. Huseby, E.S., Crawford, F., White, J., Marrack, P., and Kappler, J.W. (2006). Interface-disrupting amino acids establish specificity between T cell receptors and complexes of major histocompatibility complex and peptide. Nat. Immunol. *7*, 1191–1199. https://doi.org/10.1038/ni1401.

55. Birnbaum, M.E., Mendoza, J.L., Sethi, D.K., Dong, S., Glanville, J., Dobbins, J., Ozkan, E., Davis, M.M., Wucherpfennig, K.W., and Garcia, K.C. (2014). Deconstructing the peptide-MHC specificity of T cell recognition. Cell *157*, 1073–1087. https://doi.org/10.1016/j.cell.2014.03.047.

56. Carson, R.T., Vignali, K.M., Woodland, D.L., and Vignali, D.A. (1997). T cell receptor recognition of MHC class II-bound peptide flanking residues enhances immunogenicity and results in altered TCR V region usage. Immunity *7*, 387–399. https://doi.org/10.1016/S1074-7613(00)80360-X.

57. Huseby, E.S., White, J., Crawford, F., Vass, T., Becker, D., Pinilla, C., Marrack, P., and Kappler, J.W. (2005). How the T cell repertoire becomes peptide and MHC specific. Cell *122*, 247–260. https://doi.org/10.1016/j.cell.2005.05.013.

58. Wang, P., Sidney, J., Kim, Y., Sette, A., Lund, O., Nielsen, M., and Peters, B. (2010). Peptide binding predictions for HLA DR, DP and DQ molecules. BMC Bioinf. *11*, 568. https://doi.org/10.1186/1471-2105-11-568.

59. Wang, P., Sidney, J., Dow, C., Mothé, B., Sette, A., and Peters, B. (2008). A systematic assessment of MHC class II peptide binding predictions and evaluation of a consensus approach. PLoS Comput. Biol. *4*, e1000048.

60. Jensen, K.K., Andreatta, M., Marcatili, P., Buus, S., Greenbaum, J.A., Yan, Z., Sette, A., Peters, B., and Nielsen, M. (2018). Improved methods for predicting peptide binding affinity to MHC class II molecules. Immunology *154*, 394–406. https://doi.org/10.1111/imm.12889.

61. Nielsen, M., Lundegaard, C., and Lund, O. (2007). Prediction of MHC class II binding affinity using SMM-align, a novel stabilization matrix alignment method. BMC Bioinf. *8*, 238. https://doi.org/10.1186/1471-2105-8-238.

62. Nielsen, M., and Lund, O. (2009). NN-align. An artificial neural network-based alignment algorithm for MHC class II peptide binding prediction. BMC Bioinf. *10*, 296. https://doi.org/10.1186/1471-2105-10-296.

63. Nelson, R.W., Beisang, D., Tubo, N.J., Dileepan, T., Wiesner, D.L., Nielsen, K., Wüthrich, M., Klein, B.S., Kotov, D.I., Spanier, J.A., et al. (2015). T cell receptor cross-reactivity between similar foreign and self peptides influences naive cell population size and autoimmunity. Immunity *42*, 95–107. https://doi.org/10.1016/j.immuni.2014.12.022.

64. Woodruff, M.C., Kim, E.H., Luo, W., and Pulendran, B. (2018). B cell competition for restricted T cell help suppresses rare-epitope responses. Cell Rep. *25*, 321–327.e3. https://doi.org/10.1016/j.celrep.2018.09.029.

65. Allen, C.D.C., Okada, T., and Cyster, J.G. (2007). Germinal-center organization and cellular dynamics. Immunity *27*, 190–202. https://doi.org/10.1016/j.immuni.2007.07.009.

66. Shulman, Z., Gitlin, A.D., Weinstein, J.S., Lainez, B., Esplugues, E., Flavell, R.A., Craft, J.E., and Nussenzweig, M.C. (2014). Dynamic signaling by T follicular helper cells during germinal center B cell selection. Science *345*, 1058–1062.

67. Dustin, M.L. (2014). Review what counts in the immunological synapse? Mol. Cell *54*, 255–262. https://doi.org/10.1016/j.molcel.2014.04.001.

68. Mayer, C.T., Gazumyan, A., Kara, E.E., Gitlin, A.D., Golijanin, J., Viant, C., Pai, J., Oliveira, T.Y., Wang, Q., Escolano, A., et al. (2017). The microanatomic segregation of selection by apoptosis in the germinal center. Science *358*, eaao2602. https://doi.org/10.1126/science.aao2602.

69. Jacob, J., Kassir, R., and Kelsoe, G. (1991). In situ studies of the primary immune response to (4-hydroxy-3-nitrophenyl)acetyl. I. The architecture and dynamics of responding cell populations. J. Exp. Med. *173*, 1165–1175. https://doi.org/10.1084/jem.173.5.1165.

70. Nguyen Ba, A.N., Cvijović, I., Rojas Echenique, J.I., Lawrence, K.R., Rego-Costa, A., Liu, X., Levy, S.F., and Desai, M.M. (2019). High-resolution lineage tracking reveals travelling wave of adaptation in laboratory yeast. Nature *575*, 494–499. https://doi.org/10.1038/s41586-019-1749-3.

71. Zost, S.J., Lee, J., Gumina, M.E., Parkhouse, K., Henry, C., Wu, N.C., Lee, C.C.D., Wilson, I.A., Wilson, P.C., Bloom, J.D., et al. (2019). Identification of antibodies targeting the H3N2 hemagglutinin receptor binding site following vaccination of humans. Cell Rep. *29*, 4460–4470.e8. https://doi.org/10.1016/j.celrep.2019.11.084.

72. Finney, J., Yeh, C.H., Kelsoe, G., and Kuraoka, M. (2018). Germinal center responses to complex antigens. Immunol. Rev. *284*, 42–50. https://doi.org/10.1111/imr.12661.

73. Cohen, A.A., Gnanapragasam, P.N.P., Lee, Y.E., Hoffman, P.R., Ou, S., Kakutani, L.M., Keeffe, J.R., Wu, H.-J., Howarth, M., West, A.P., et al. (2021). Mosaic nanoparticles elicit cross-reactive immune responses to zoonotic coronaviruses in mice. Science *371*, 735–741. https://doi.org/10.1126/science.abf6840.

74. Yassine, H.M., Boyington, J.C., Mctamney, P.M., Wei, C.J., Kanekiyo, M., Kong, W.P., Gallagher, J.R., Wang, L., Zhang, Y., Joyce, M.G., et al. (2015). Hemagglutinin-stem nanoparticles generate heterosubtypic influenza protection. Nat. Med. *21*, 1065–1070. https://doi.org/10.1038/nm.3927.

75. Kanekiyo, M., Wei, C.J., Yassine, H.M., Mctamney, P.M., Boyington, J.C., Whittle, J.R.R., Rao, S.S., Kong, W.P., Wang, L., and Nabel, G.J. (2013). Self-assembling influenza nanoparticle vaccines elicit broadly neutralizing H1N1 antibodies. Nature *499*, 102–106. https://doi.org/10.1038/nature12202.

76. Nelson, S.A., Richards, K.A., Glover, M.A., Chaves, F.A., Crank, M.C., Graham, B.S., Kanekiyo, M., and Sant, A.J. (2022). CD4 T cell epitope abundance in ferritin core potentiates responses to hemagglutinin nanoparticle vaccines. NPJ Vaccines *7*, 124. https://doi.org/10.1038/s41541-022-00547-0.

77. Locci, M., Havenar-Daughton, C., Landais, E., Wu, J., Kroenke, M.A., Arlehamn, C.L., Su, L.F., Cubas, R., Davis, M.M., Sette, A., et al. (2013). Human circulating PD-1+CXCR3-CXCR5+ memory Tfh cells are highly functional and correlate with broadly neutralizing HIV antibody responses. Immunity *39*, 758–769. https://doi.org/10.1016/j.immuni.2013.08.031.

78. Havenar-daughton, C., Lee, J.H., and Crotty, S. (2017). Tfh cells and HIV bnAbs , an immunodominance model of the HIV neutralizing antibody generation problem. Immunol. Rev. *275*, 49–61. https://doi.org/10.1111/imr.12512.

79. Hu, J., Havenar-Daughton, C., and Crotty, S. (2013). Modulation of SAP dependent T:B cell interactions as a strategy to improve vaccination. Curr. Opin. Virol. *3*, 363–370. https://doi.org/10.1016/j.coviro.2013.05.015.

80. Aldhamen, Y.A., Appledorn, D.M., Seregin, S.S., Liu, C.j.J., Schuldt, N.J., Godbehere, S., and Amalfitano, A. (2011). Expression of the SLAM family of receptors adapter EAT-2 as a novel strategy for enhancing beneficial immune responses to vaccine antigens. J. Immunol. *186*, 722–732. https://doi.org/10.4049/JIMMUNOL.1002105.

81. Jardine, J., Julien, J.P., Menis, S., Ota, T., Kalyuzhniy, O., McGuire, A., Sok, D., Huang, P.S., MacPherson, S., Jones, M., et al. (2013). Rational HIV immunogen design to target specific germline B cell receptors. Science *340*, 711–716. https://doi.org/10.1126/science.1234150.

82. Ekiert, D.C., Bhabha, G., Elsliger, M.A., Friesen, R.H.E., Jongeneelen, M., Throsby, M., Goudsmit, J., and Wilson, I.A. (2009). Antibody recognition of a highly conserved influenza virus epitope. Science *324*, 246–251. https://doi.org/10.1126/science.1171491.

83. Amitai, A., Sangesland, M., Barnes, R.M., Rohrer, D., Lonberg, N., Lingwood, D., and Chakraborty, A.K. (2020). Defining and manipulating B cell immunodominance hierarchies to elicit broadly neutralizing antibody responses against influenza virus. Cell Syst. *11*, 573–588.e9. https://doi.org/10.1016/j.cels.2020.09.005.

84. Meakin, P. (1984). Diffusion-limited aggregation in three dimensions: results from a new cluster-cluster aggregation model. J. Colloid Interface Sci. *102*, 491–504. https://doi.org/10.1016/0021-9797(84)90252-2.

85. Southwood, S., Sidney, J., Kondo, A., del Guercio, M.F., Appella, E., Hoffman, S., Kubo, R.T., Chesnut, R.W., Grey, H.M., and Sette, A. (1998). Several common HLA-DR types share largely overlapping peptide binding repertoires. J. Immunol. *160*, 3363–3373.

STAR★METHODS

KEY RESOURCES TABLE

REAGENT or RESOURCE	SOURCE	IDENTIFIER
Deposited data		
Simulation data	This paper; Mendeley Data	https://doi.org/10.17632/2kt95vthcs.1
Software and algorithms		
MATLAB	MathWorks	https://www.mathworks.com/products/matlab.html
Simulation and analysis algorithm in MATLAB	This paper; Mendeley Data	https://doi.org/10.17632/2kt95vthcs.1
Other		
Mice immunization data in Figure 4	Caradonna et al.[35]	https://doi.org/10.1101/2022.12.01.518697

RESOURCE AVAILABILITY

Lead contact

Further information and requests for resources and reagents should be directed to and will be fulfilled by the lead contact, Arup Chakraborty (arupc@mit.edu).

Materials availability

This study did not generate new unique reagents.

Data and code availability

- Simulation data have been deposited on Mendeley Data: https://doi.org/10.17632/2kt95vthcs.1 and are publicly available.
- All original code has been deposited on Mendeley Data: https://doi.org/10.17632/2kt95vthcs.1 and is publicly available.
- Any additional information required to reanalyze the data reported in this paper is available from the lead contact upon request.

METHOD DETAILS

Affinity maturation simulation algorithm

As described in the main text, we simulate in-silico germinal centers in which B cells capture antigen and then compete for help by T cells in each cycle, for 28 cycles. The stochastic GC simulation is repeated 1,000 times. We keep track of the following quantities: the number of GC B cells that target each epitope (rsH3, rsH4, or rsH14 off-target B cells or RBS-directed B cells), the binding affinities of the GC B cells, the mutations that are carried by the RBS-directed B cells, and the probabilities of positive selection of RBS-directed B cells at each round. For reporting the RBS-directed B cell fractions (see Figure 4), all B cells from the 1,000 GCs are first pooled together, and then the fraction is calculated.

The amounts and types of antigens captured by the B cells are determined by simulating the immunological synapse between the B cell and the FDC. BCRs first cluster with antigens, then internalize them by applying force (see sections model development and Antigen capture depends on immunogen design and cross-reactivity of B cells in the main text). Then, the probability of positive selection by T cells is determined based on the amount and diversity of the antigens captured by the B cell, relative to other competing B cells (see Equation 9 and the associated description in the main text). We provide further detail and analyses of these steps below.

Simulation of antigen capture

The immunological synapse is modeled as a circle of radius 0.5 μm divided up into lattice points with an interval of 10 nm that can be occupied by the antigens and BCRs. No two homotypic molecules are allowed on the same lattice site, but a BCR and an antigen molecule can occupy the same site. To begin the simulation, 120 BCRs and 120 antigen molecules are randomly distributed on the lattice sites. During the clustering phase, BCR and antigen molecules diffuse freely. In each time step, each molecule randomly chooses one of the four neighboring sites, then moves to it with the probability of,

$$p_{move} = \frac{4D\Delta t}{l^2}$$

where $D = 5\times10^4$ nm^{2}s^{-1} is the diffusion constant for both antigen and BCR[50] and $l = 10$ nm is the lattice size. For clusters of BCRs and antigens, only those containing up to 3 molecules are allowed to diffuse and the diffusion coefficient is reduced to D/M where M is the number of molecules in a cluster.[84] The move is completed if the new sites are not blocked for the diffusing molecules. If any of the new sites are already occupied or are outside the boundary of the immunological synapse, the move is not accepted and the simulation continues to the next step.

When the distance between a BCR and an antigen molecule is either 0 or 1 lattice site, they can form a bond, as described in the main text. When several free epitopes on the antigen molecules are recognized by the BCR, one is randomly chosen upon binding. The sizes of clusters stabilize within a few seconds of simulation time (data not shown), so we simulate the clustering phase for 10 seconds.

When the extraction phase begins, BCRs and any antigen molecules bound to them stop diffusing, but free antigen molecules still diffuse. A pulling force is applied to each BCR, which affects the antigen extraction as described in the main text (see Equations 6–8). The simulation terminates once all BCRs are internalized, and the number and types of internalized antigen molecules are calculated.

The simulation of antigen capture is computationally intensive, so repeating it for thousands of B cells for each round of affinity maturation is impractical. Therefore, we first run the antigen capture simulations to determine the mapping between the binding affinities of a B cell and the amount of antigen it captures, then use this mapping to quickly determine how much antigen each B cell captures during the affinity maturation simulations. To obtain the mapping for a strain-specific B cell, we run 30 independent simulations of antigen capture for each value of binding affinity between -13.8 and $-20.8\ k_BT$ with an interval of $0.5\ k_BT$. The mean amount of antigen captured is determined at each point. This affinity range covers the limits of B cell affinities relevant in our affinity maturation simulation. The amount of antigen captured by a B cell is determined from standard linear interpolation using the two nearest points to its binding affinity. For the RBS-directed B cells, we run the antigen capture simulations for a set of grid points on a three-dimensional grid, where each axis corresponds to the binding affinity towards one rsHA component, ranging between -13.8 and $-20.8\ k_BT$ with an interval of $0.5\ k_BT$. The amount of antigen captured by a given B cell is obtained from a standard trilinear interpolation using the eight nearest points.

Selection by T cells

The main text describes how the probability of positive selection by T cells depends on both the amount and the diversity of the captured antigens (see Equation 9). Here, we provide a mathematical analysis of why immunization with the cocktail antigen favors cross-reactive B cells in the early GC when T cell help is permissive, but not when it is stringent (see Figure 4).

The low-affinity RBS-directed B cell precursor and off-target B cells capture similar amounts of total antigen. For simplicity, let us assume that the amounts of antigen captured are equal. That is, $A_1 + A_2 + A_3 = A_{1,off}$ where $A_1, A_2, A_3 > 0$ are the amounts of the three variants captured by an RBS-directed B cell, and $A_{1,off}$ is the amount captured by an off-target B cell that, without loss of generality, is assumed to target only the first variant.

Equation 9 is a monotonically increasing function of the numerator $\sum_k \left(\frac{T_k}{N_{B,k}}\right)\cdot\left(\frac{A_{ki}}{\langle A_k\rangle}\right)^x$. Therefore, to understand how the positive selection probability of the RBS-directed B cell compares with that of the off-target B cell, we will compare q_{RBS}, defined as $\sum_k \left(\frac{T_k}{N_{B,k}}\right)\cdot\left(\frac{A_{ki}}{\langle A_k\rangle}\right)^x$ and q_{off}, defined as $\left(\frac{T_1}{N_{B,1}}\right)\left(\frac{A_{1,off}}{\langle A_1\rangle}\right)^x$.

In our model, we assume that equal numbers of T cells target the epitopes from each of the three rsHA variants. That is, $T_1 = T_2 = T_3$. Also, each off-target B cell is randomly assigned the target variant with equal probability. Since there is a relatively large number of founder B cells (99 off-target B cells), we can approximate that the number of B cells that capture each variant are equal, i.e. $N_{B,1} = N_{B,2} = N_{B,3}$.

Also, the mean amount of antigen k internalized by B cells that recognize antigen k, $\langle A_k\rangle$, is equal for all k at the beginning of the GC because all B cells have the same affinity. Since GCs contain thousands of B cells, this equality also holds well due to symmetry even when B cells begin to mutate, at least in early GCs. Taken together, the following equality holds.

$$\frac{q_{RBS}}{q_{off}} = \frac{\left(\frac{T_1}{N_{B,1}}\right)\left(\frac{A_1}{\langle A_1\rangle}\right)^x + \left(\frac{T_2}{N_{B,2}}\right)\left(\frac{A_2}{\langle A_2\rangle}\right)^x + \left(\frac{T_3}{N_{B,3}}\right)\left(\frac{A_3}{\langle A_3\rangle}\right)^x}{\left(\frac{T_1}{N_{B,1}}\right)\left(\frac{A_{1,off}}{\langle A_1\rangle}\right)^x} = \frac{A_1^x + A_2^x + A_3^x}{A_{1,off}^x} = \frac{A_1^x + A_2^x + A_3^x}{(A_1 + A_2 + A_3)^x}$$

To show that the RBS-directed B cells are favored for positive selection when T cell help is permissive, we will prove the following inequality:

$$A_1^x + A_2^x + A_3^x > (A_1 + A_2 + A_3)^x \text{ if } 0 < x < 1$$

Consider the function $f(a_1, a_2, a_3) = a_1^x + a_2^x + a_3^x - (a_1 + a_2 + a_3)^x$ defined for positive real numbers a_1, a_2, a_3. The partial derivatives are always positive if $0 < x < 1$:

$$\frac{\partial f}{\partial a_i} = x a_i^{x-1} - x(a_1 + a_2 + a_3)^{x-1} > 0 \text{ for } i = 1, 2, 3$$

because $a_i < a_1 + a_2 + a_3$ and $x - 1 < 0$.

Assume that there exists $A_1, A_2, A_3 > 0$ such that $f(A_1, A_2, A_3) = s \leq 0$. Then, for any a_1, a_2, a_3 such that $a_1 \in (0, A_1), a_2 \in (0, A_2), a_3 \in (0, A_3)$, the following inequality must be true:

$$f(a_1, a_2, a_3) < f(A_1, A_2, A_3) = s \leq 0$$

However, f is a continuous function and $\lim_{a_1 \to 0, a_2 \to 0, a_3 \to 0} f(a_1, a_2, a_3) = 0$. Therefore, there must exist $\delta > 0$ such that

$$|f(a_1, a_2, a_3) - 0| < |s| \quad \text{for all } a_1, a_2, a_3 \in (0, \delta)$$

which is contradictory.

Therefore, $q_{RBS} > q_{off}$ when $x < 1$, and by simple extension, $\frac{p_{max} q_{RBS}}{1 + q_{RBS}} > \frac{p_{max} q_{off}}{1 + q_{off}}$. That is, despite capturing the same amount of antigen, the RBS-directed B cell has a higher probability of positive selection because of capturing diverse T cell epitopes. By similar analysis, it can be shown that when $x > 1$ the opposite is true, and the RBS-directed B cells have a lower probability of positive selection.

T cell epitope prediction and comparison

T cell epitopes in the rsH3, rsH4, and rsH14 antigens (Figure 3) as well as in the rabbit serum albumin and human serum albumin (Figure S2) are predicted with IEDB MHCII binding prediction tool. For the comparison of rabbit serum albumin and human serum albumin, we excluded the peptides whose 9-mer core sequences were also found in mouse serum albumin, since such peptides would not be immunogenic in mice.[64] The following settings are used: Prediction Method – IEDB recommended 2.22; Select species/locus – mouse, H-2-I; Select MHC allele – H2-I-A^b; Select length – 15. The predicted peptides are sorted by the percentile rank given by the IEDB tool, and the peptides in the top 20 percentile are chosen for the pairwise comparisons of the epitopes in different variants. This value corresponds to roughly ~3000 nM predicted half-maximal inhibitory concentration (IC50) value. We choose this cutoff to be comprehensive because most immunogenic MHC II T cell epitopes have an IC50 value under 1,000 nM.[85] The 9-mer cores associated with the peptides, predicted by the smm_align method, are then used for the pairwise comparisons.

QUANTIFICATION AND STATISTICAL ANALYSIS

The stochastic GC simulation was repeated 1,000 times for each parameter tested, with unique seeds for the random number generator in MATLAB. For reporting the RBS-directed B cell fractions, all B cells from the 1,000 GCs were first pooled together, and then the fraction was calculated (see Figure 4 legend). The stochastic antigen capture simulation was repeated 30 times for each parameter tested, and the mean value of the antigen captured was reported (see Figure 2B legend).